Direct measurements of E × B flow and its impact on edge turbulence in the CASTOR tokamak using an optimized Gundestrup probe *)

J. Gunn

Association EURATOM-CEA sur la Fusion Controlee, DRFC, CEA Cadarache, France

J. Stöckel, J. Adámek, I. Ďuran, J. Horáček, M. Hron, K. Jakubka, L. Kryška, F. Žáček

Department of Applied Physics, Ghent University, Ghent, Belgium

G. Van Oost

Institute of Plasma Physics, Association EURATOM/IPP.CR, Prague, Czech Republic

Received 12 October 2001

New experimental evidence of the correlation between edge sheared **E**×**B** flow and reduction of turbulence has been measured in the CASTOR tokamak ($R = 0.4\,\mathrm{m}$, $a = 0.085\,\mathrm{m}$, $B_T = 1\,\mathrm{T}$). A biasing electrode is placed at the separatrix in a configuration which has demonstrated strongly sheared electric fields and consequent improvement of the global particle confinement. A set of movable electrostatic probes (rake, Langmuir, Gundestrup, and rotating Mach) provide redundant, simultaneous measurements of poloidal flow, toroidal flow, electron temperature, density, and radial electric field with high temporal resolution and at the same poloidal location. Particular effort has been made in the optimization of the Gundestrup probe collector geometry in order to reduce the relative uncertainty of Mach number measurements in plasmas with weak flow ($M_\parallel, M_\perp < 0.1$). The measurements from the rake, Gundestrup, and rotating Mach probes give three independent radial profiles of **E**×**B** shear in ohmic and biased modes. Good agreement is obtained both for the profile shape and its absolute magnitude. The plasma flows, especially the poloidal **E**×**B** drift velocity, are strongly modified in the sheared region, reaching Mach numbers as high as half the sound speed. The corresponding shear rates ($\approx 5 \times 10^6\,\mathrm{s}^{-1}$) derived from both the flow and electric field profiles are in excellent agreement and are at least an order of magnitude higher than the growth rate of unstable turbulent modes as estimated from fluctuation measurements. In addition, we compare the measured **E**×**B** ion mass flow with the phase velocity of fluctuations moving poloidally across the Gundestrup collectors. Given the poloidal separation of the collecting plates and the sampling frequency (5 MHz), the maximum detectable phase velocity turns out to be rather modest compared to the measured bulk poloidal flow speed. Therefore the two quantities are only compared when the poloidal speed is low; in that case, they show similar behaviour in response to the applied bias.

*) Presented at the 4th Europhysics Workshop "Role of Electric Fields in Plasma Confinement and Exhaust", Funchal, Madeira, Portugal, June 24–25, 2001

1 Introduction: the optimized Gundestrup probe

1.1 Comparison between the Gundestrup probe and the rotating Mach probe

Gundestrup probes [1] are used to measure ion flows in magnetized plasmas. The standard design consists of six to twelve conducting pins mounted around an insulating housing in order to obtain a significant variation of the angle between the magnetic field and the probe surface. According to fluid and kinetic modeling, the current density collected by each pin is largely determined by the Bohm–Chodura boundary condition [2]. Despite the rigour of the physics formulation, the precision of flow measurements by Gundestrup probes has so far been limited to large parallel and perpendicular Mach numbers ($|M_{\|}|, |M_{\perp}| > 0.1$). This is because slight angular misalignments and finite gap width between the pins and the housing cause non-negligible uncertainty of the individual effective collecting areas.

The Gundestrup probe design has been improved ("Ideal Gundestrup Probe", IGP) and tested in order to render it attractive for flow measurements even in unbiased edge plasmas. The ion collecting surface is a nearly continuous cylindrical conductor (a copper tube of diameter 11.7 mm) divided into eight segments separated by 0.2 mm gaps, as shown in Fig. 1. The segments are fastened to an insulating boron nitride tube. The collecting area, determining the radial resolution (2.2 mm), is defined by an insulating quartz sleeve (not shown in the picture) that is slightly shorter than the central conductors. The eight collectors are biased negatively into ion saturation in order to construct polar diagrams with good temporal resolution. A single Langmuir probe tip is installed at the front end of the IGP; its voltage is swept to obtain current–voltage characteristics and calculate the plasma parameters in the proximity of the probe. All signals are sampled at 1 MHz.

Fig. 1. Ideal Gundestrup probe.

This optimized design has been validated in the CASTOR tokamak ($R = 40$ cm, $a = 8.5$ cm, $B_T = 1$ T). The poloidal and toroidal flows are measured simultaneously at the same radius by the IGP and rotating Mach probe (RMP) [3]. Polar diagrams of the ion saturation current measured by the IGP and RMP are compared in Fig. 2. The data are recorded during the biasing period of the discharge. Both probes are positioned inside the separatrix, at the radial electric field maximum, and

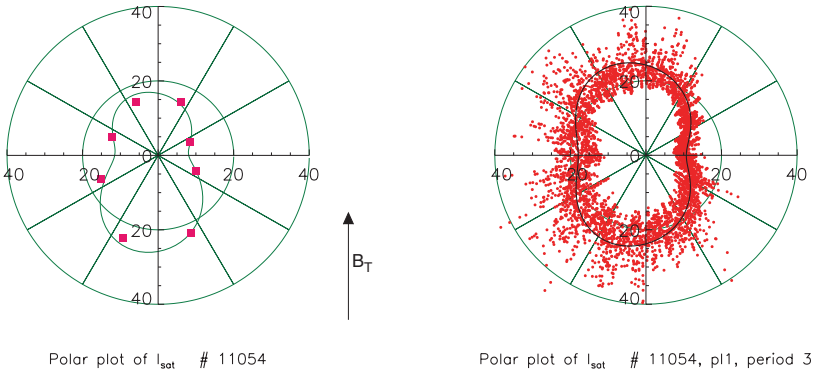

Fig. 2. Polar diagrams of the ion saturation current as measured in the same shot by the IGP (left) and the RMP (right) located inside the separatrix ($r = 70\,\mathrm{mm}$). The experimental points are fitted to the KD model [2] (solid lines). #11054.

consequently are not connected to any material element of the discharge chamber.

It is well seen that experimental data are reasonably fitted by the fluid model [3] and the resulting Mach numbers are shown in Table 1.

Table 1.

	$M_{\parallel}$	$M_{\perp}$
IGP	-0.2	-0.18
RMP	$+0.0$	-0.24

From this table and even from the visual inspection of the diagrams, a different shape of the polar ion current distribution, in particular in the toroidal direction, is apparent. It is possible that toroidal asymmetries of the ion flow could exist in the CASTOR tokamak. Local recycling from different objects in the SOL (for example the biasing electrode or the poloidal limiter), plus viscous propagation of parallel flow from the various presheaths into the core could lead to such asymmetries. One can not exclude that the difference in the $M_{\parallel}$ determination is partially caused by a misalignment of the probes with respect to the magnetic field lines [2].

Alternatively, the probe data are processed by the model developed by H. Van Goubergen [4]. An advantage of this method is that it provides an analytic formula for the ratio of upstream and downstream currents. However, only four of the eight segments are used for processing of the raw data. Consequently, we have only two points from which we derive the Mach number using linear regression. So, an extraordinary signal from one segment (due to arcing, large density fluctuations, etc) corrupts the result. This limitation arises because the model assumes that perpendicular transport consists uniquely of coherent flow (the $\mathbf{E}\times\mathbf{B}$ drift), ignoring flux due to finite Larmor radii. Theoretically the current on the top segments where the magnetic field is nearly parallel should approach zero, but in reality, the current is enhanced due to deflection of ion orbits in the magnetic presheath. On the other

hand, the KD model uses data from all eight segments and consequently is not so sensitive to extraordinary events.

1.2 Investigation of interference between neighbouring segments

One of the open questions related to functioning of the standard Gundestrup probes is whether the signal of one particular tip is influenced by its neighbourhood. The ion current to one collector could possibly depend on whether the adjacent surfaces are insulators, floating conductors, or biased. The novel design, presented here has the capability to answer this question. The following experiment has been performed: one collector's voltage is swept ($U = 100\,\mathrm{V}$, $f = 1\,\mathrm{kHz}$) and the I–V characteristics are measured. The remaining tips are either kept floating, or negatively biased and their signals are recorded. The sequence is repeated for all eight collectors. The main results of this experimental series are presented in Fig. 3.

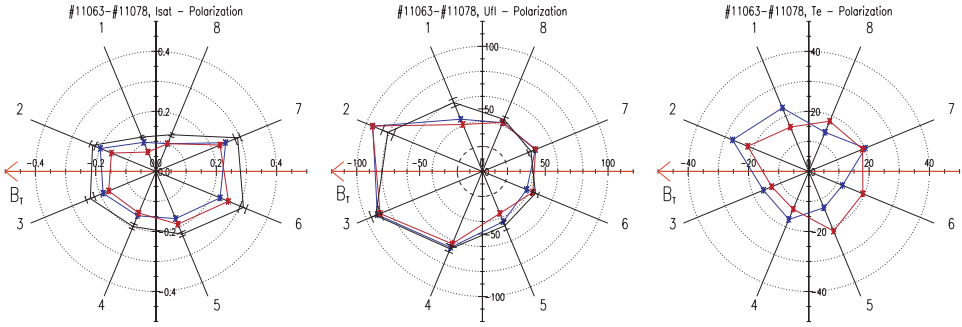

Fig. 3. Polar diagrams of the swept IGP. From left to right: Ion saturation current, floating potential, electron temperature. $M_\perp = -0.23$, $M_\parallel \approx 0$.

The black lines show the standard IGP diagram, when all tips measure either I_{sat} or U_{float}. These diagrams are averaged over eight shots and the error bars are shown. Red lines correspond to the case when one tip is swept, while the remaining tips measure the ion saturation current. Blue lines connect points of the swept pin when the remaining tips are floating. It is evident from the figure that the swept and "standard" polar diagrams of I_{sat} and U_{float} are practically of the same shape. This indicates an independence of the pin signal on its neighbourhood. Interestingly, a systematic difference between biased and floating configurations seems to be apparent in the diagram of T_{e}. However, more statistics are necessary for definite conclusions.

This measurement is carried out in polarized discharges with a large $M_\perp$, but $M_\parallel \approx 0$, as apparent from the polar diagram of I_{sat}. It is interesting to note that diagram of U_{float} is asymmetric just in the parallel direction, i.e. turned by about 90°. The floating potential is more negative on the electron side of the IGP (the plasma current has the same orientation as the toroidal magnetic field), indicating the possible existence of a small population of non-thermal electrons [5].

2 Correlation between poloidal flow and radial electric field

2.1 Experimental arrangement

The toroidal lay-out of the key elements of the experiment is shown in Fig. 4. The electrode is located at the separatrix ($r_\mathrm{b} = 75\,\mathrm{mm}$), and is positively biased with respect to the vacuum vessel. It has been shown recently [6] that such a biasing scheme effectively modifies the radial electric field not only in the scrape-off layer, but also in front of the electrode in the region of open magnetic field lines. The radial profile of the floating potential is monitored at the plasma edge by a rake

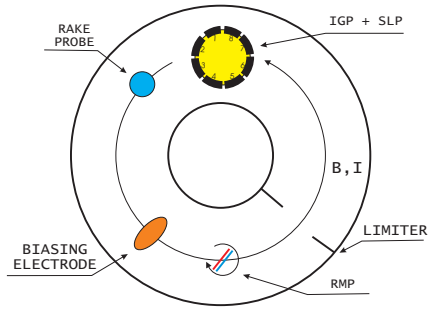

Fig. 4. Lay-out of the key elements of the experiment. The IGP and RMP are moved radially on a shot-to-shot basis. The connection lengths: biasing electrode & RMP $\approx 28\,\mathrm{cm}$, biasing electrode & IGP $\approx 98\,\mathrm{cm}$.

probe [7] to derive the radial electric field in the edge plasma. All these tools are located at the same poloidal angle (at the top of the torus) to assure their respective radial positioning with a sufficient precision. The IGP and RMP are moved radially between shots to construct profiles of density, temperature, plasma potential, and parallel and perpendicular Mach numbers. The collecting plates of the RMP are biased into ion saturation and the rotation period is roughly 5 ms. The segments of the IGP are also biased negatively to measure the polar distribution of ion current, and the small Langmuir probe tip in front of the housing is swept to obtain the plasma parameters.

2.2 Perpendicular Mach number versus the radial electric field

The first series of shots was devoted to the systematic investigation of the relation between the $\mathbf{E}\times\mathbf{B}$ and ion flow velocities in biased discharges. To that end, the IGP was located at two distinct radial positions in front of and behind the biasing electrode, in the region of highest radial electric field ($r = 70\,\mathrm{mm}$ and $r = 85\,\mathrm{mm}$), deduced from the radial profile of the floating potential measured by the means of the rake probe, see Fig. 5.

It is seen from the figure, the gradient of the floating potential is enhanced with biasing ($U_\mathrm{b} = +100\,\mathrm{V}$) at both sides of the electrode, i.e. in the SOL as well as

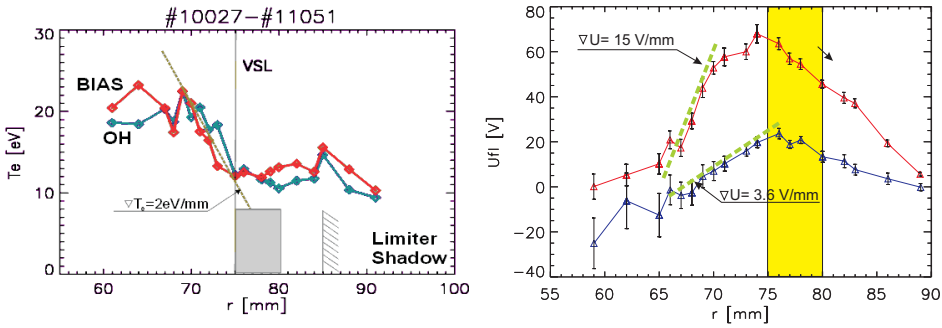

Fig. 5. Radial profile of electron temperature (left) and floating potential (right) in ohmic and biased phase of discharges measured by the single Langmuir probe located at the top of the IGP. Position of the separatrix is at $r = 75$ mm, which corresponds to the location of the top of the biasing electrode. The radial extent of the biasing electrode is marked by the yellow box.

inside the separatrix. The radial electric field is calculated following the expression

$$E_\mathrm{r} = -(\nabla U_\mathrm{fl} + \alpha \nabla T_\mathrm{e})$$

where the factor α is rather uncertain in magnetized plasmas [8] and ranging from 1.3 to 3. As seen from the left panel of Fig. 5, the actual radial profile of the electron temperature must be taken into account because of rather large local gradients of

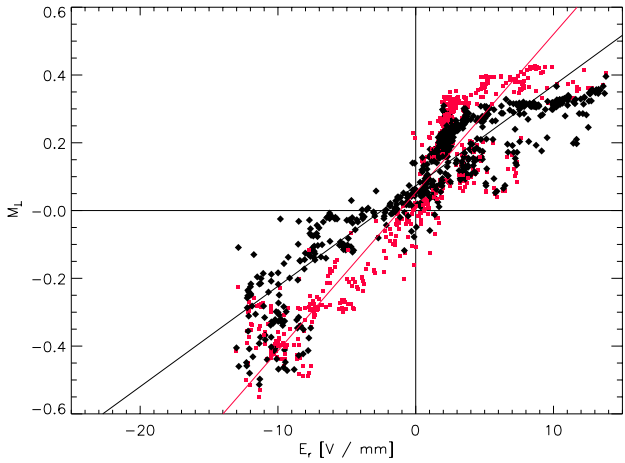

Fig. 6. Perpendicular Mach number versus the radial electric field. The red points correspond to Mach numbers deduced from the KD model [3], while the blue marks are calculated using the VG model [4]. $E_\mathrm{r} < 0$ — IGP is inside separatrix, $E_\mathrm{r} > 0$ — IGP is in the SOL

the electron temperature observed within the separatrix ($\nabla T_\mathrm{e} \approx -2\,\mathrm{V/mm}$), but also in the SOL ($-1\,\mathrm{V/mm}$). Note the similar shape of $T_\mathrm{e}(r)$-profiles in ohmic as well as at separatrix biasing regimes.

Series of discharges at different biasing voltage have been performed. The resulting dependency of the perpendicular Mach number on the radial electric field is shown in Fig. 6. It is evident from the figure that the perpendicular Mach number is proportional to the magnitude of the radial electric field. The slope of the curves is determined by the ion sound velocity, which is either $c_\mathrm{s} = v_{\mathbf{E}\times\mathbf{B}}/M_\perp \approx 21.5\,\mathrm{km/s}$ (KD-fit) or 32 km/s (VG-fit). It is interesting to compare this experimental value with the expression

$$c_\mathrm{s} = \sqrt{\frac{k(ZT_\mathrm{e} + \gamma T_\mathrm{i})}{m_\mathrm{i}}} \approx 9.8 \times 10^3 \sqrt{ZT_\mathrm{e} + \gamma T_\mathrm{i}}\,,$$

which gives for the experimentally measured electron temperature 16 eV a significantly higher value, $\approx 40\,\mathrm{km/s}$, even in the case of $T_\mathrm{i} = 0$, $Z = 1$. This may indicate that the actual value of the electron temperature is less than that measured from I–V characteristics of the single Langmuir probe. This may appear, for example, if the edge plasma is non-maxwellian, and contains a few percent of suprathermal electrons [5]. It is clear that this observation needs further analysis.

2.3 Fluctuation and flow velocities

In the second experimental series, the measured ion mass flow is compared with the phase velocity of fluctuations moving poloidally across the Gundestrup collectors (see Fig. 7). The ion mass flow is measured by the standard arrangement of the Gundestrup probe, i.e., signals of all the segments are digitized at a standard sampling rate ($1\,\mu$s/sample), then averaged over the time interval 0.5 ms. From these data, the perpendicular Mach number of the ion flow is derived. Simultaneously, the

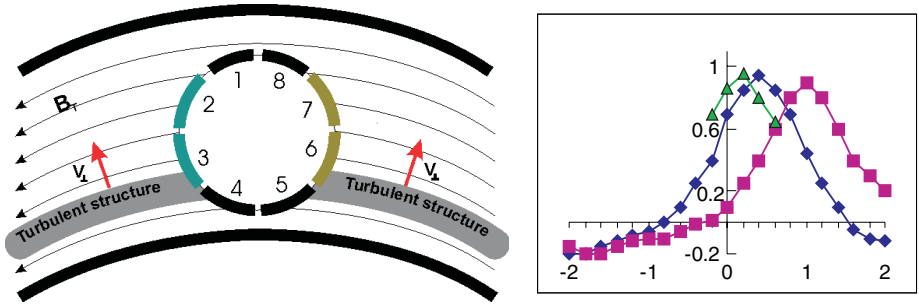

Fig. 7. Left: Principle of comparison of flow and fluctuation measurements. Right: Shape of the cross-correlation function of fluctuating signals of the segments nearly perpendicular to the magnetic field lines (schematically).

signals from the most upstream and downstream pairs of the segments, i.e. 2–3 and 6–7 are recorded faster, at a sampling rate of 5 MS/s. Then, the cross-correlation function is calculated and the transit time of a poloidally localized structure across the corresponding segments is deduced from the shift of its maximum (see the right panel in Fig. 7). The phase velocity of fluctuations is calculated as the ratio of the distance between the adjacent segments (4.5 mm in our particular case) and the transit time. It has to be emphasized that time delays by one sample have been considered as statistically uncertain and consequently not taken into account in the calculation of fluctuation velocities. Thus, the maximum velocity, which can be determined in this way is about 11 km/s.

Two examples of the evolution of the fluctuation velocities in the combined OH–Bias–BiasLH–LH–OH discharges is shown in Fig. 8. The biasing period is 4 ms (from $t = 8$ to $t = 12$ ms). The LH phase of the discharge is also 4 ms long, starting at $t = 10$ ms.

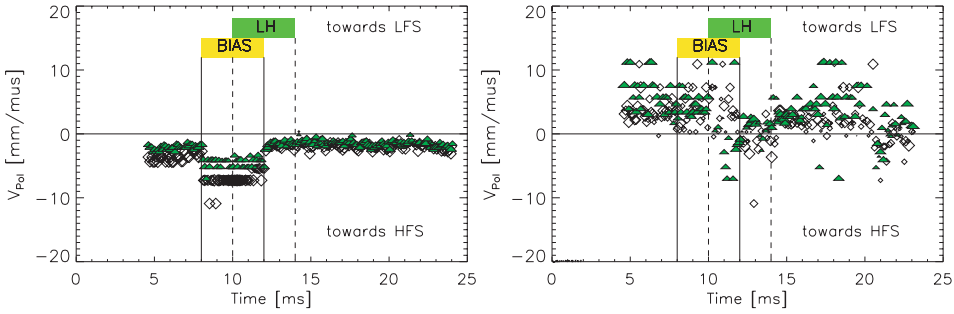

Fig. 8. Evolution of the phase velocity of fluctuations as measured simultaneously by the pair of segments 2–3 (diamonds) and 6–7 (triangles). Left: IGP is positioned in the SOL; Right: IGP is inside the separatrix.

The left panel shows the evolution in the SOL. It is seen that the upstream and downstream pairs yield roughly the same values of the fluctuation velocity, $\approx$ 2 km/s. The velocity increases during the biasing phase, as expected, but a difference between pairs is already visible. Nevertheless, if the details are not taken into account, the physical picture agrees well with the generally accepted model of edge turbulence, in which the turbulent structures are "flutes", localized in the poloidal and radial direction and associated with a particular magnetic surface. The right panel shows the evolution inside the last closed flux surface. Here, the propagation is reversed, as expected. However, the data are much more scattered then in the previous case and the pairs of segments measure different values of the phase velocity. Sometimes, the upstream pair measure fluctuations propagation in the opposite direction then the downstream pair. This last mentioned effect is even more evident when the IGP is in the proximity of the separatrix. We conclude from these observations thatthe parallel wavenumber of the turbulent structures increases inside the separatrix. Possibly, the structures live their own life independently on

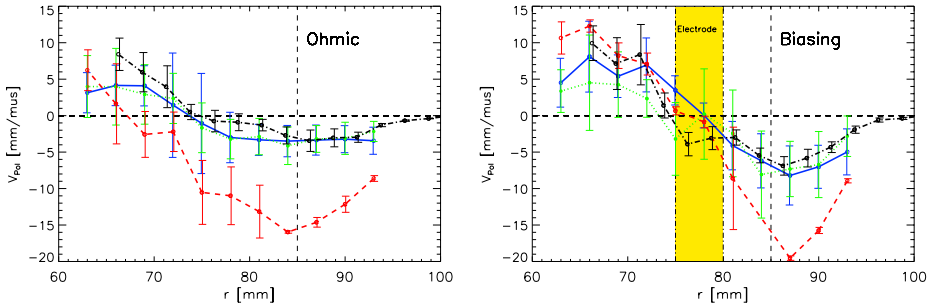

Fig. 9. Radial profile of fluctuation velocities (blue and green lines), and flow velocity (red line) measured by the IGP. The black line is the **E**×**B** velocity deduced from the rake probe data. Left: ohmic phase of the discharge. Right: Biased phase of the discharge.

the bulk plasma. Maybe some structures may leave the magnetic surface.

In Fig. 9 we compare four measurements of the poloidal velocity deduced from (1) the IGP polar diagrams, (2) the phase velocity of structures moving across the upstream segments, (3) the phase velocity of structures moving across the downstream segments, and (4) the **E**×**B** drift speed calculated from the radial electric field profile. In both the ohmic and bias phases of the discharge, all methods give the same sign of the flow, and roughly the same inversion radius. It is evident from the figure that the flow and fluctuation velocities are comparable within the separatrix (in particular with biasing), while a large discrepancy in their magnitudes is measured in the SOL. These measurements (1–3) are obtained simultaneously on the IGP probe, so the disagreement cannot be due to toroidal asymmetries. A clear agreement of fluctuation and **E**×**B** velocities (measurement 4) is observed. As mentioned in Section 2.2, the difficulty with the flow measurements is that one must define the ion sound speed. Since the ion temperature is not known, this definition is arbitrary. Furthermore, the fitting constants derived from the

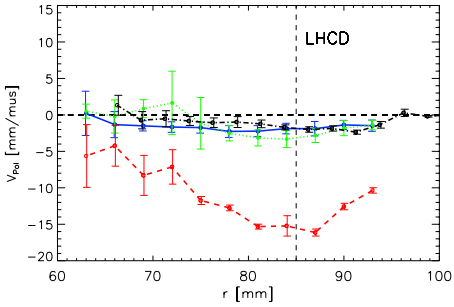

Fig. 10. Radial profile of fluctuation and flow velocity measured by the IGP during the LH phase of the discharge.

fluid models are calculated assuming equal ion and electron temperatures. The constant for parallel flow is known to change with the ion-to-electron temperature ratio [9], so it is probable that the constant for perpendicular flow also changes. Kinetic calculations for different ion temperatures would be useful to address this problem [2].

The edge plasma can be also effectively modified by injection of Lower Hybrid Waves, as illustrated in Fig. 10 that shows an example of such impact. The radial profile of the floating potential is flat during the LH phase of the discharge. Consequently, the fluctuation and flow velocities are close to zero in a broad range of radii. However, the fluctuation and flow velocities differ significantly. Again, we suspect problems due to the uncertain ion sound speed, especially in the presence of fast electrons generated by LH.

3 Conclusions

It is demonstrated that separatrix biasing and lower hybrid wave injection provide non-intrusive tools to modify flows and electric fields on closed magnetic flux surfaces. The plasma flows, especially the poloidal $\mathbf{E}\times\mathbf{B}$ drift velocity, are strongly modified in the sheared region, reaching Mach numbers as high as half the sound speed. It is also shown that the Ideal Gundestrup Probe offers a unique possibility to study the link between the ion flows and poloidal propagation of turbulent structures simultaneously. The good correlation between the measured phase velocity and the $\mathbf{E}\times\mathbf{B}$ drift indicates that the turbulent structures are "frozen" into the poloidally rotating plasma. This picture agrees with measurements of floating potential fluctuation by a 2D matrix of probes [10].

References

[1] C.S. MacLatchy et al.: Rev. Sci. Instrum. **63** (1992) 3923.

[2] J.P. Gunn et al.: Phys. Plasmas **8** (2001) 1995.

[3] K. Dyabilin et al.: in *Proc. 27th EPS Conf. on Contr. Fusion and Plasma Phys.*, Budapest 2000, EPS, Mulhouse, ECA **24B** (2000) 1653.

[4] H. Van Goubergen et al.: Plasma Phys. Contr. Fusion **41** (1999) L17.

[5] P.C. Stangeby: Plasma Phys. Contr. Fusion **37** (1995) 1031.

[6] G. Van Oost et al.: in *Proc. ITC-11 TOKI 2000*, to appear in J. Plasma Fusion Res. Series.

[7] J. Stöckel et al.: Plasma Phys. Contr. Fusion **41** (1999) A577.

[8] R. Schrittwieser et al.: in *Proc. 28th EPS Conf. on Contr. Fusion and Plasma Physics*, Funchal 2001, in print.

[9] K.-S. Chung and I. H. Hutchinson: Phys. Rev. A **38** (1988) 4721.

[10] E. Martines et al.: in *Proc. 28th EPS Conf. on Contr. Fusion and Plasma Physics*, Funchal 2001, in print.